New Acrylate Co-Polymer Membrane Synthetized by Photo-Polymerization Technique for Lead (II) Ion-Selective Electrode

[1*]Sagir Alva, [2,6]Rika S. Utami, [1]Melny Andrian, [1]Arsyad Widinugroho, [3]Aiman S. A. Aziz, [4]Siti A. Hasbullah, [1,5]Deni S. Khaerudini, [1]Dafit Feriyanto, [2]Kee S. Loh and [2]Edy H. Majlan

Received 29/03/2023; accepted 08/05/2023
https://doi.org/10.4152/pea.2024420503

[1]Mechanical Engineering Department, University Mercu Buana, West Jakarta 11650, Indonesia
[2]Fuel Cell Institute, University Kebangsaan Malaysia, 43600, UKM Bangi, Selangor Darul Ehsan, Malaysia
[3]Flexible Electronics Lab, MIMOS Berhad 57000 Kuala Lumpur, Malaysia
[4]Department of Chemical Sciences, Faculty of Science and Technology, University Kebangsaan Malaysia, 43600 UKM Bangi, Selangor, Malaysia
[5]Research Center for Advanced Materials, National Research and Innovation Agency (BRIN), Kawasan Puspitek Serpong, South Tangerang 15314, Indonesia
[6]Electrical Engineering and Computer Department, Faculty of Engineering, University Syiah Kuala, Banda Aceh 23111, Indonesia
*Corresponding author: sagir.alva@mercubuana.ac.id

Abstract
A novel p(THFA-co-HEMA) membrane based on acrylate CP was successfully synthesized through PP technique, and applied into Pb-ISE (Pb-ISE). THFA optimum composition was HEMA 9:1 (TH91), with a T_g of -6.5 ºC. The structure of p(THFA-co-HEMA) was characterized using FTIR. The Pb-ISE sensor showed remarkable calibration measurement in the range from 0.1 to 10^{-6} M, with a LOD of 7.59 x 10^{-7} M, and it has obeyed a Nernstian number of 30.5 mV/dec. In addition, the fabricated Pb-ISE sensors showed fairly good selectivity coefficients of several types of ions, such as K^+ (-6.53 ± 0.11), Na^+ (-6.35 ± 0.16), NH_4^+ (- 6.76 ± 0.11), Mg^{2+} (-12.15 ± 0.13), Ca^{2+}(12.12 ± 0.14), Cu^{2+} (-4.33 ± 0.11) and Cd^{2+} (-6.43 ± 0.17), and an effective function in the pH range from 3 to 8. The resulting response time was quite good, 6.7 sec, with a change of 27.5 mV for a decade. The Pb-ISE sensor also showed validation results equivalent to AAS standard method, where the corresponding data with real samples produced values of 9.3 ± 1.9 and 9.2 ± 2.0 ppm and 275.5 ± 10.3 and 277.7 ± 4.0 μg/g, for CREW and CRMS, respectively.

Keywords: acrylate membrane; ISE; p(THFA-co-HEMA); Pb(II); PP.

Introduction•

ISE is a transducer or sensor comprising a polymeric host membrane and sensing components, which converts the specific ion activities or ion Ct in a solution into an electrical E. The polymeric membrane plays an essential role in ISE construction [1-4]. In general, the membrane has two main roles. Firstly, it acts as

• The abbreviations list is in pages 348-349.

a supporting matrix capable to retain its sensing components, such as liphophilic salts, ionophores and plasticizers, which serves to reduce the membrane T_g [5]. Secondly, the membrane also acts as a separator matrix between the aqueous sample and the ISE transducer surface or internal layer [1, 6-7]. Fig. 1 shows the structural construction for cationic ISE.

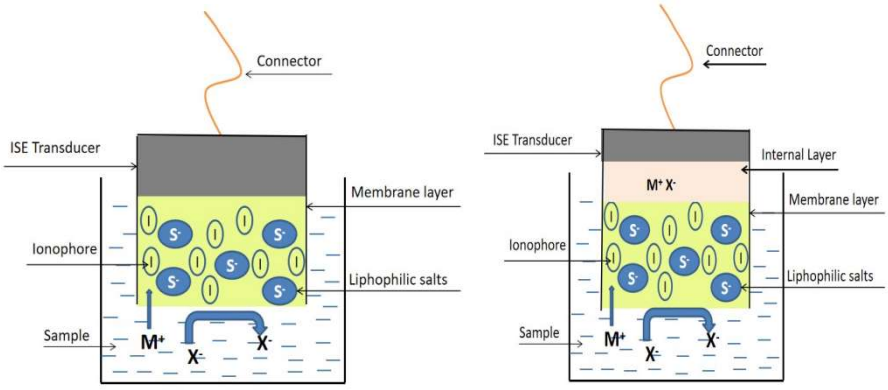

Figure 1: Illustration of an ISE sensor structure **(a)** without and **(b)** with internal layer.

In ISE development, there are several important characteristics of its membrane, prior to the sensor fabrication process. The polymeric membrane used in ISE must have stable properties, so that it does not easily dissolve in the sample or undergo a redox reaction. Furthermore, the membrane must possess low or non-toxic properties, considering that some of the specimens used are medical samples, of which measurements are conducted invasively and used for blood vessels. In addition, the membrane must also be able to work well with all the sensor components needed for ISE fabrication, such as lipophilic salts, ionophores, plasticizers and organic solvents [6-7]. Additionally, polymeric T_g from -40 to 15 ºC is ideal, so that ions transfer from the sample onto the membrane occur properly, and the sensing components inside the membrane do not easily leach-off [2, 6-8]. Hence, the challenge to produce a desirable polymeric host matrix compatible with Pb (II) ions detection and measurement for Pb-ISE is of great interest [3].

Pb (II) ion is one of the heavy metal ions that is very toxic for the environment and living beings, and even disrupts human health through exposure to in-trace amounts. According to WHO, the maximum traceability limit of Pb (II) ion in drinking water is 10 µg/, or even lower, at 7.2 µg/L^2, as recommended by European WFD [2, 9-10]. Pb (II) ion accumulation can cause serious damage to human organs, such as liver, bones, nervous system, brain, and other important tissues, which in turn can bring death [11]. Typically, human exposure to Pb (II) ion occurs through food chain systems, air pollution and workplace environmental conditions [12-13].

Conventionally, PVC membrane is commonly used in Pb-ISE sensors fabrication [14-18]. However, this type of membrane has high T_g value, which requires plasticizers addition to reduce it. This helps to increase the polymer backbone segmental motion and generate free volume for sensing components mobility in the polymer structure [2, 6, 8]. Plasticized membranes are not recommended for medical applications, especially for invasive ISE sensors in blood vessels, since they are

generally toxic, and if they leach, they will certainly poison blood [6, 19]. In addition, PVC-ISE fabrication main disadvantage is its long and complicated process. PVC membranes normally have longer evaporation times for the drying process to form thin films. Generally, the evaporation process takes from 12 to 24 h. Another disadvantage of the PVC membrane is that it has poor adhesion on the electrode surface, from which it can peel off. To overcome this issue, a membrane clamping procedure is usually performed. However, ISE small size or SPE shape certainly involve complex fabrication and design processes [2, 6, 8].

The limitations shown by PVC membrane have encouraged researchers to continue to develop films that are suitable for producing Pb-ISE sensors. Another polymer host membrane developed for ISE is PHXA [20]. PHXA advantage is its ability to function as a sensing membrane, even though without plasticizers addition. However, PHXA is still unideal, due to its poor selectivity and complicated fabrication process, which takes up to 1 week of drying time.

Another alternative sensing membrane is based on polyacrylate, which has several advantages over previous reported membranes, such as: being able to function without plasticizers; having available variable monomers with which their mechanical properties can be adjusted; adhering well on the surface; and allowing for its preparation either through TP or PP [3, 21]. Pb-ISE sensors development based on polyacrylate has been reported by previous researchers, such as [22], who used pIDA. This membrane can function well for a Pb-ISE sensor, even without plasticizers. However, such approach has fundamental drawbacks, such as the preparation process involving a TP process that requires many solvents, multiple steps and longer heating and drying times, which reach 24 h. The same unfavourable fabrication process was carried out by [23], using a thin CP membrane made of MB.

The long preparation time will certainly lead to higher Pb-ISE fabrication costs. So, another alternative method to produce a rapid polymeric host membrane within a few min is PP [2, 8, 24]. A Pb-ISE sensor based on PP of polyacrylate has been developed by [24], using pBA and CP of pBA-HEMA. Both Pb-ISE sensors showed very good responses, especially the one fabricated with CP of pBA-HEMA. However, since the developed pBA and pBA-HEMA membranes are very soft and slightly sticky [2, 8], their mishandling will rupture them, and they may stick on the beaker glass walls during measurements.

Another alternative is to use pTHFA membrane PP, which was developed by [2]. This Pb-ISE sensor has shown better mechanical properties than those of pBA, but its linear measurement ranges only up to 10^{-5} M. Thus, Pb-ISE sensor performance can still be improved. Herein, HEMA monomer addition on Pb (II) sensing membrane was investigated. HEMA is a hydrophilic acrylate membrane that is commonly applied as an ISE sensor inner layer. Typically, CP of HEMA membranes are often used as supporting matrices to immobilize biological materials for bio-sensor applications. CP of HEMA with excellent hydrophilic properties helped to promote ion transports from the sample to the electrode or transducer surface [25-26].

Based on the above description, Pb-ISE fabrication process was herein carried out using PP technique, wherein THFA-co-HEMA membrane CP was used as fabrication material. HEMA monomers addition was expected to improve the

performance of THFA based Pb-ISE. The research included the testing of THFA-co-HEMA CP structure and T_g value, by FTIR and DSC. Additionally, Pb-ISE sensors performance was tested on their linear range, LOD, selectivity and pH effect. Validation was tested through AAS method, using artificial solutions and real samples.

Methodology

Instrumentations

The equipment used in this study included Corrtest CS350 potentiostat, Pt electrode and SCE (Wuhan Corr Test Instrument Corp. Ltd.), 9V battery, Ag-SPE (Scrint Print, Sdn Bhd-Malaysia), UV-box exposure (Huanyu Instrument), TGA/DSC (DTA PT1600 Linsesis) and FTIR (Thermoscientific Nicolet iS-10).

Materials

The chemicals used in this study were THFA and HEMA monomers (Merck), Pb ionophore (IV), HDDA (as cross-linker agent), DMPP (as photo-initiator) and KTpClPB (Sigma-Aldrich). The salts material used were $Pb(NO_3)_2$, KCl, NaCl, NH_4Cl, Tris-HCl, $MgCl_2.6H_2O$, $CaCl_2.2H_2O$, $CuCl_2.2H_2O$, $Cd(NO_3)_2.4H_2O$, HCl 36% solution and also solid NaOH (Merck).

Experimental

THFA-co-HEMA CP synthesis and characterization

Initially, pTHFA-co-HEMA CP were prepared by mixing THFA, HEMA, DMPP and HDDA monomers with the composition shown in Table 1. Then, the monomers were homogeneously mixed until a clear solution was formed.

Table 1: Variants in pTHFA-co-HEMA CP composition.

CP	THFA (mg)	HEMA (mg)	HDDA (mg)	DMPP (mg)
TH95	95	5	0.016	1
TH91	90	10	0.016	1
TH82	80	20	0.016	1
TH73	70	30	0.016	1
TH64	60	40	0.016	1

Each monomer variant was placed on the microscope glass slide, and PP process was carried out for 3.5 min, under continuous N atmosphere in the UV-exposure box. The thin film formed on the glass slide surface was then slowly removed and stored in a sample bottle, for structural analysis, using FTIR. In addition to structural testing, T_g measurements were also carried out using a TGA/DSC device in the formed film. Furthermore, films that met T_g value from -40 to -15 ºC were selected as polymers for Pb-ISE sensor fabrication.

Pb(II)-ISE preparation and performance test

For preparing Pb-ISE sensor, firstly, Ag/AgCl electrode, which was produced through electroplating technique in a 0.5 M KCl solution, for 30 sec., was used as the sensor platform. Ag-SPE platform was connected to the positive (+) terminal,

and Pt (RE) was connected to the 9 V battery negative (-) terminal. After the electroplating process, a brownish-brown AgCl thin layer was formed in the Ag-SPE surface. Then, the formed Ag/AgCl electrode was washed with deionized water and dried with tissue paper.

The second preparation step was to form an inner pHEMA layer on the Ag/AgCl electrode surface, by adding 0.1 µL HEMA on it. Then, the PP process was carried out for 1.5 min, in a UV-exposure box, with continuous N gas flow, after which a thin pHEMA film layer was formed. The layer was then further hydrated by a droplet of 0.01 M $Pb(NO_3)_2$, for 15 min. Then, the remaining solution was gently wiped with tissue paper.

In the third preparation step, 100 µL of each selected CP variant was mixed with 1 mg KTpClPB and Pb Ionophore (IV), at 1:1 mole ratio. Then, the mixture was vigorously mixed until a clear liquid was formed. 3 µL of each CP mixture was drop coated on the pHEMA layer surface. Subsequently, PP process was carried out for 3.5 min, in N gas flow atmosphere, after which a new pTHFA-co-HEMA CP film layer was formed, and the Pb-ISE sensor was ready for characterization. The Pb-ISE sensor was conditioned in a 0.01 M $Pb(NO_3)_2$ solution, for 30 min. Nernstian numbers and the linear range of measurements were carried out. The best characterized CP composition proceeded for performance tests, such as selectivity coefficient, pH effect and validation. The validation testing was carried out by measuring the artificial solutions and real samples Ct using the Pb-ISE sensor, and comparing it with the NSA standard method (SNI number 06-6989.8-2004).

Results and discussion

Structure analysis of p(THFA-co-HEMA) CP

The newly synthesized p(THFA-co-HEMA) CP sensing structural analysis was further characterized before being used as sensing host matrix. This novel acrylate CP has never been reported before. In this study, structural analysis was carried out using FTIR. The sample used was the TH82 CP, as a representative of the five synthesized acrylate polymer combinations, since, in principle, the molecular structure of the variants was identical. The analysis results of the p(THFA-co-HEMA) CP structure are shown in Fig. 2.

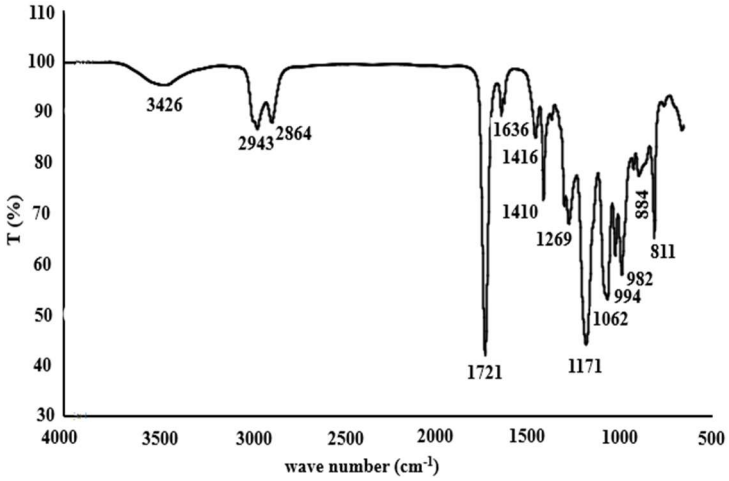

Figure 2: FTIR spectrum of p(THFA-co-HEMA) CP.

Based on Fig. 2, it seems that the FTIR spectrum produced seven peaks in the region from 1400 to 4000 cm^{-1}, which is the main area. In addition, there were also seven peaks in the band below 1400 $cm^{-1,}$ which is a fingerprint area that serves as supporting data for FTIR analysis [27]. In the area of 3426 cm^{-1}, there was a broad peak, which is a stretching band of -OH functional group. In addition, -OH is 1636 cm^{-1} peak, which is the bending band of this group. Meanwhile, in the area of 2800-3000 cm^{-1}, there are sharp twin peaks at positions 2943 and 2864 cm^{-1}. Both peaks were stretched from asymmetric and symmetrical C-H groups derived from methylene and methyl. At 1721 cm^{-1}, there is a very sharp peak, which is C=O functional group stretching. Around 1400 cm^{-1}, there are two peaks at 1416 and 1410 cm^{-1}, which correspond to C-H bending from the methyl and α-methyl groups, respectively. The α-methyl functional group is also at 811 cm^{-1}. In the areas of 1269 and 1171 cm^{-1} are -C-O-C bending. Meanwhile, at 994 cm^{-1}, C-O originates from furan ring. 1062, 982 and 884 cm^{-1} bands are typical of the acrylate band [28-33].

Based on the characterization that was obtained from FTIR analysis, as previously described above, CP structure formed from the PP process with UV light is depicted in Fig. 3.

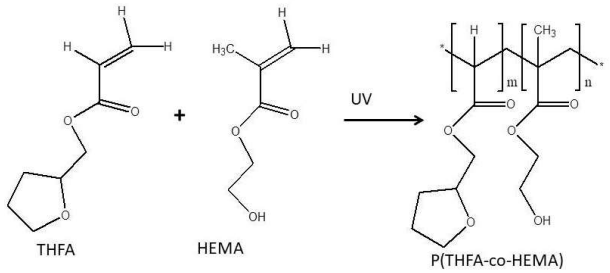

Figure 3: Formation reaction of p(THFA-co-HEMA) CP through PP process.

DSC analysis

A membrane with T_g mechanical properties of novel p(THFA-co-HEMA) was determined using DSC analysis. A significant T_g value, which affected ions movement in the membrane used during Pb ion measurement process, was important to minimize the developed Pb-ISE sensor fouling tendency. [2, 6-8]. In this study, DSC measurements were carried out on five composition variants and carried out within a T range from -30 to 100 ºC, of which results are shown in Table 2.

Table 2: T_g values of p(THFA-co-HEMA) CP variants prepared by PP technique.

Membrane	THFA (mg)	HEMA (mg)	T_g estimation (ºC)	T_g measurement (ºC)
TH9.50.5	95	5	-8	-10.5
TH91	90	10	-3	-6.5
TH82	80	20	7	5.1
TH73	70	30	17	17.7
TH64	60	40	27.2	26.3

The heating rate used in DSC test was 10 ºC/min. DSC test T range sorting was based on THFA and HEMA T_g values, which were -13 and 87 ºC, respectively [34-35]. The synthesized acrylate CP T_g value was in the range of both monomers.

This condition is in accordance with Fox Eq., which explains that T_g value of a CP will be proportional to the weight fraction (ω) of each monomer [34, 36-37].

$$T_{gCP} = (T_{gA} \times \omega_A) + (T_{gB} \times \omega_B) \quad (1)$$

Table 2 shows that T_g generated from DSC measurements did not differ greatly from the results of calculations based on Eq. (1). It also shows that HEMA monomers changed T_g value of the CP. The measurement results revealed that, with higher Ct of HEMA, T_g value of the resulting CP increased, in accordance with Fox Eq. predictions. This is inseparable from the influence of α-CH_3 derived from HEMA monomers [28]. Based on the test results, TH95, TH91 and TH82 membranes were selected for Pb-ISE sensor fabrication, since they have required T_g values, which range from -40 to 15 ºC [2, 6-8].

Pb-ISE response

Using the potentiometric technique, a ISE sensor membrane WE was coupled with a standard RE, to form a complete sensor measurement system. In principle, potentiometric analysis measures V that occurs between an ISE sensor with a RE vs. the ion activity logarithm without a current. Potentiometric techniques measurements follow Nernstian Eq:

$$E = const + \frac{2.303RT}{F z_A} \log a_A \quad (2)$$

where E is the V between the ISE sensor and the RE, and R is the universal gas constant (8.314 J / K mol). Absolute T is at 298 K. F is a Faraday number (96,435 C/mol), z_A is A ion charge and a_A is A ion activity [38]. In this study, A ion used was Pb^{2+}.

For assessing Pb-ISE sensor response, a total of three replicate sensors were fabricated from each formulated CP variants (TH9.50.5, TH91 and TH82). All Pb-ISE electrodes were tested in a $Pb(NO_3)_2$ solution ranging from 0.1 to 10^{-9} M. Based on the results shown in Table 3, all the designed CP for Pb-ISE sensors displayed a Nernstian number from 28.2 to 29.7 mV/dec. This is close to the divalent ions theoretical Nernstian number from 24.6 to 34.6 mV/dec [2, 39]. Therefore, Pb-ISE sensors response is depicted by Eq. (3). Fig. 4 shows that all sensor responses did not significantly change at lower Ct, from 10^{-6} to 10^{-9} M Pb^{2+}.

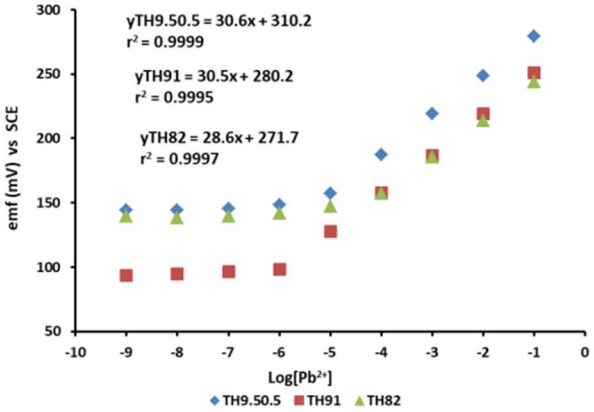

Figure 4: Pb-ISE response of three different p(THFA-co-HEMA) CP ratios in the Ct of $Pb(NO_3)_2$ solution.

In the area below LOD, ISE sensors response was constant, even with changes in the Ct of the test solution. This LOD region was calculated based on the intersection point between the linear and the constant regions [40]. This was not only because the number of ions at low Ct is increasingly limited [2], but also due to the membrane hydrophilicity. This hydrophilicity affects ions movement in the membrane [25, 40-41].

$$E = E^{o} + 29.6\ mV\ Log\ a_{Pb2+} \quad (3)$$

Table 3: Performance of Pb-ISE sensor with variations in the P(THFA-co-HEMA) CP membrane an in the Ct of $Pb(NO_3)_2$ solution.

Membrane	Slope (mV/dec)	Linear range (M)	LOD (M)	R^2
TH9.50.5	30.6	0.1 - 10^{-5}	3.80 x 10^{-6}	0.9999
TH91	30.5	0.1 - 10^{-6}	7.59 x 10^{-7}	0.9995
TH82	28.6	0.1 - 10^{-4}	2.40 x 10^{-5}	0.9997

Although all three sensors have good Nernstian numbers, they exhibited different linear ranges, as shown in Table 3. Synthesized TH91 has the longest linear range among the three membrane types, followed by TH95, while the shortest was for TH82. The linear range difference is influenced by HEMA monomers in the acrylate polymers structure. In principle, HEMA is a hydrophilic acrylate based monomer, with a T_g value higher than that of the THFA monomer (87 ºC) [34-35]. With these characteristics, HEMA monomers with a certain ratio will cause response variance in Pb-ISE sensors [25].

On the other hand, the sensor with TH95 showed a linear response in the range from 0.1 to 10^{-5} M. A similar finding was reported by a previous research that only used pTHFA membrane for the Pb-ISE sensor development [2], because 5% w/w HEMA monomer was not enough to increase Pb-ISE sensor linear range. However, 10% w/w HEMA in TH91 membrane increased Pb-ISE sensor range from 0.1 to 10^{-6} M, due to the monomer hydrophilic nature that also gave CP that property. This change was due to ions diffusion from the sample, which enabled the Ag/AgCl transducer response to their penetration in the membrane located on the sensor surface [25].

20% w/w HEMA decreased Pb-ISE sensor linear range from 0.1 to 10^{-4} M, which was linked to acrylate CP increased hydrophilicity. This created conditions for more Pb^{2+} ions and also a small number of interfering and counter ions to enter in the membrane, which affected Pb-ISE sensor response [25, 42]. The increased hydrophilic nature also allowed for membrane components, such as ionophore and lipophilic salts, to be more easily released into the sample solution. This situation disrupted the membrane components balance, which is one of the main features in ISE sensors fabrication [2]. Based on data shown in Fig. 4 and Table 3, the Pb-ISE sensor with TH91 was selected for further testing.

Pb-ISE performance

Herein, the optimum sensor result obtained for TH91 was further tested, since this membrane had the most extensive measurement range compared to the other two.

The detailed testing of Pb-ISE sensor performance included selectivity coefficient, response time and pH effect. Selectivity testing describes the sensor ability to respond to the target analyte, without being influenced by contaminant ions in the test sample. It is a crucial test, since real samples generally contain various ions types [44, 46]. There are several methods for testing selectivity coefficient, such as MSM and SSM [13, 46-48]. SSM selectivity test was performed, due to its simple and rapid procedure. It is done by measuring Pb^{2+} and K^+, Na^+, NH_4^+, Mg^{2+}, Ca^{2+}, Cu^{2+} and Cd^{2+} interfering ions V values, at the same Ct of 0.1 M [49]. Furthermore, the selectivity coefficient value was calculated in Eq. 4, of which results are shown in Table 4.

$$LogK^{pot}_{a,b} = \frac{(E_B - E_A)z_A F}{2.303RT} + \left(1 - \frac{z_A}{z_B}\right)\log a_A \quad (4)$$

where E_B is confounding ion E value, E_A is primary ion E, zA is primary ion charge, z_B is interfering ion charge, F is Faraday number (96,485 C/ mole), R is universal gas constant (8.314 j/K mole (298 K)) and a_A is target ion Ct (at a T of 25 ºC) [2].

Table 4: Pb-ISE sensor coefficient selectivity (Log $K^{pot}_{a, b}$) with interfering ions (n=3).

Interfering ion	Log $K^{pot}_{a, b}$
K^+	-6.53 ± 0.11
Na^+	-6.35 ± 0.16
NH_4^+	-6.76 ± 0.11
Mg^{2+}	-12.15 ± 0.13
Ca^{2+}	-12.12 ± 0.14
Cu^{2+}	-4.33 ± 0.11
Cd^{2+}	-6.45 ± 0.17

Table 4 shows that Pb-ISE sensor incorporated with p(THFA-co-HEMA) had good selectivity against other interfering cations, which makes it advantageous as a membrane matrix for potentiometric sensors and results in high sensitivity towards Pb^{2+}. The sensing matrix was incorporated into Pb (IV) ionophore, which was used for Pb^{2+} ion recognition. Pb (IV) selective ionophore was derived from amides, which gives it superior selectivity, even in the presence of interfering cations. This result is in agreement with reports from literature on Pb sensor development [2, 16, 37, 50-52].

The response time is the period required by Pb-ISE sensor to instantly react to changes in the sample Ct, until it reaches an equilibrium point, following Le Chartlier principle. This equilibrium point is an indication that Pb-ISE sensor has reached its stability point marked by changes of <1 mV/min [2, 40, 52]. Hence, this test was conducted by measuring the Pb-ISE sensor V in a $Pb(NO_3)_2$ solution, at an initial low Ct of 0.001 M. Subsequently, 0.1 M $Pb(NO_3)_2$ was added to the sample solution, to achieve final Ct of 0.01 M. In Fig. 5, at the measurement start and, after 30 sec., the sensor had a E value of 217.7 and 217.6 mV, respectively.

The result shows that, during the first 30 sec., Pb-ISE sensor was fairly stable in the 0.001 M test solution. At 32.3 sec., 0.1 M $Pb(NO_3)_2$ was added to the test solution, and the sensor E value instantaneously changed from 218.5 mV, until a new equilibrium point was achieved, at 39 sec., with a final E value of 246.0 mV.

So, the calculated response time required for Pb-ISE sensor was 6.7 sec., with the increased E value of 27.5 mV. The obtained response time was quite good and proportional to the one provided by Pb-ISE sensors developed by previous researchers [14-15, 17, 53]. Good response time was inseparable from low T_g value and synthesized p(THFA-co-HEMA) membrane hydrophilicity. It was conclusively shown that Pb^{2+} ions easily diffused from the sample onto the Ag/AgCl transducer sensor surface, which is shown in Fig. 1 [2-6, 25, 42].

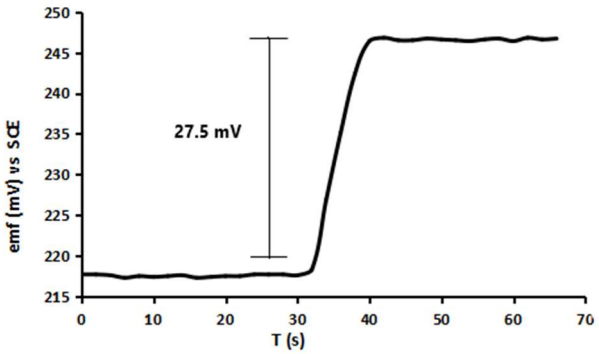

Figure 5: Pb-ISE sensor response time graph in 0.001 to 0.01 M Pb $(NO_3)_2$.

The main challenge faced by researchers in Pb-ISE development is that the metal formation is strongly influenced by pH [2]. In this study, pH testing was carried out at pH 2-10, using three Ct of the Pb $(NO_3)_2$ solution, from 0.1 to 10^{-3} M, as shown in Fig. 6. The overall sensor response with different Ct of $Pb(NO_3)_2$ shows that pH 2 had a slightly lower E value than of that at pH 3-8. At pH 3-8, Pb-ISE sensor E value was not very different. However, at pH 9-10, there was a change in E value signal for all the test solutions. The condition at pH < 3 was due to Pb (IV) ionophore, which underwent a deprotonation process that affected Pb-ISE sensor response [12, 50, 54]. When pH > 8, the sample environmental conditions became more alkaline, which caused some Pb ions turning into $Pb(OH)_2$ deposits. These deposits decreased Pb^{2+} ions Ct in the sample, which lowered E value [14, 18, 53]. These findings suggest that Pb-ISE sensor developed from p(THFA-co-HEMA) membrane effectively works in the pH range from 3 to 8.

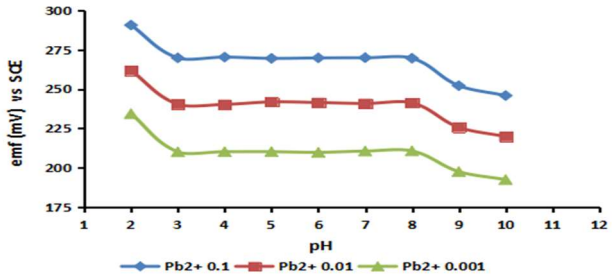

Figure 6: Response of Pb-ISE sensor at different pH, in 0.1, 0.01 and 0.001 M $Pb(NO_3)_2$ solutions.

In general, Pb-ISE sensor based on p(THFA-co-HEMA) membrane showed comparable performance to some Pb-ISE developed by several previous researchers, as seen in Table 5.

Table 5: Pb-ISE performance based on p(THFA-co-HEMA) membrane comparison with previous studies.

Slope (mV/dec)	Dynamic range (M)	LOD (M)	pH range	Response time (sec.)	Ref
25.79	0.1 - 10^{-6}	4 x 10^{-7}	5 -7.2	10	14
26.49 ± 0.7	0.1 - 10^{-6}	7.6 x 10^{-7}	4 -7	<10	15
29.0 ± 0.2	2x10^{-3} - 2x10^{-9}	4 x 10^{-10}	2 - 4.8	<10	16
27.65	0.1 -10^{-7}	-	3 - 7	10	17
30 ± 0.2	0.1 - 10^{-5}	4 x 10^{-6}	4 - 8	45	55
29.8	0.1 - 10^{-8}	4.3 × 10^{-9}	3.5 - 7.3	5-7	56
29.1 ± 0.3	10^{-3} to 10^{-9}	6.31× 10^{-10}	3 - 9	<5	57
31.5	I0^{-2} - 10^{-8}	6.0 × 10^{-9}	2 - 8	5	58
27.25	10^{-5} -10^{-10}	< 10^{-10}	7 - 8	25	59
30.5	0.1 - 10^{-6}	7.59 x 10^{-7}	3 - 8	6.7	this work

Validation test

Electrochemical validation test is one of the most well-known methods to ensure that the developed Pb-ISE sensor performance is comparable to standard methods [14]. The standard method used in this study was NSA, as recommended by SNI 06-6989.8-2004 [2]. This validation test used two types of samples: an artificial one, with 10, 50 and 100 ppm; and a real sample that was collected from CREW and CRMS.

CREW and CRMS were selected, because Ciliwung is one of the main rivers that divides the city of Jakarta, which flows from the Mount Gede Pangrango to the Jakarta Bay. Along with CR flow, there are many urbanization community activities that dispose trash into the river, including battery waste containing many heavy metals such as Pb. In addition, especially in the estuary area, many industrial activities also dispose their waste into the river [60-62]. The sensor validation test results for artificial and real samples are shown in Table 6. In this study, the real samples used were spiked with a 50 ppm standard solution.

Table 6: Comparison of Pb^{2+} ions measurement results for artificial and real samples, using Pb-ISE sensors and AAS (n = 3).

Samples	Pb-ISE	NSA
10 ppm	10.9 ± 0.2	10.7 ± 0.4
50 ppm	52.1 ± 1.3	52.5 ± 0.9
100 ppm	103.3 ± 0.5	102.6 ± 0.7
CREW (ppm)	9.3 ± 1.9	9.2 ± 2.0
CRMS (μg/g)	275.4 ± 10.3	277.3 ± 4.0

The results indicate that Pb^{2+} ion detection using Pb-ISE sensor was comparable to that obtained using NSA standard method (SNI 06-6989.8-2004 procedure). For real water samples, the presence of other ions in Pb-ISE sensor did not significantly affect the measurement results. However, the real sample data indicated that CREW exceeded the standard water quality of 10 μg/L [2, 9], due to the extreme process of urbanization and industrial activities that occur along the river, causing waste discharge accumulation in CRM area. This data is also comparable with results from previous studies, which stated that CRM had heavy metals, such as Pb, at Ct from 8.49 to 50.96 ppm, and the sediments were from 20 to 336 μg/g [60].

The findings of this research provided insight about the CR water quality and have raised serious concern by the Jakarta local government.

Conclusions

The p(THFA-co-HEMA) CP acrylate was successfully synthesized and characterized using FTIR. This CP was applied as a supporting membrane matrix in Pb-ISE sensors fabrication. From the five variants of the proposed p(THFA-co-HEMA) CP compositions, only three have met the specifications for the Pb-ISE sensors, which included TH9.50.5, TH91 and TH82, with T_g values from -10.5 to 5.1 ºC. The best variant of the three CP was TH91, with a measurement range from 0.1 to 10^{-6} M and LOD of 4.16 x 10^{-7} M. The diffused Pb-ISE sensor showed good selectivity coefficients for several types of ions, such as K^+, Na^+, NH^{4+}, Mg^{2+}, Ca^{2+}, Cu^{2+} and Cd^{2+}. Its ideal pH was in the range from 3 to 8. Besides that, Pb-ISE sensor had fairly good response time of 6.7 sec at 27.5 mV. The sensor test with artificial solutions and real samples from CRMS provided results comparable to the NSA standard method, according to SNI 06-6989.8-2004.

Acknowledgment

The authors thank to University Mercu Buana for funding this research through the KLN research scheme with grant number 02-5/646/B-SPK/III/2020. Acknowledgments were also given to the collaborating Institutions who participated in the completion of this research such as the University Kebangsaan Malaysia who helped with the FTIR analysis, Mimos Berhad who assisted with FTIR testing, and LIPI Fisika who assisted with T_g analysis using DSC tools.

Author contributions

Sagir Alva: acted as the head of the research project and was in charge of designing research, writing, data analysis and conducting correspondence with publishers. **Rika Sri Utami**: carried out poly(THFA-co-HEMA) membrane synthesis and characterization. **Melny Andrian**: optimized membrane composition and conducted Pb-ISE testing. **Arsyad Widinugroho**: prepared real samples and conducted validation tests. **Aiman Sajidah Abd Aziz**: assisted the DSC analysis. **Siti Aishah Hasbullah**: helped to analyze Pb-ISE sensor performance and assisted in writing the manuscript. **Deni Shidqi Khaerudini**: helped to analyze FTIR. **Dafit Feriyanto**: helped to write the manuscript and administrate this research. **Kee Shyuan Loh**: helped to design membranes synthesis and characterization. **Edy Herianto Majlan**: assisted the validation testing process.

Abbreviations

AAS: atomic absorption spectrophotometry
$CaCl_2.2H_2O$: calcium chloride, dihydrate
$Cd(NO_3)_2.4H_2O$: cadmium nitrate tetrahydrate
CP: co-polymer
CR: Ciliwung river
CREW: Ciliwung river estuary water

CRMS: Ciliwung river mouth sediments
Ct: concentration
$CuCl_2.2H_2O$: copper(II) chloride dehydrate
DSC: differential scanning calorimetry
DMPP: 2,2-dimethoxy-2-phenylacetophenone
E: potential
FTIR: Fourier-transform infrared spectroscopy
HDDA: 1,6-hexanediol diacrylate
HEMA: 2-hydroxyethyl methacrylate
ISE: ion selective electrode
KTpClPB: potassium tetrakis(4-chlorophenyl)borate lipophilic salt
LOD: limit of detection
MB: methyl methacrylate-butyl acrylate
$MgCl_2.6H_2O$: magnesium chloride hexahydrate
MSM: mixed solution method
NH_4Cl: ammonium chloride
NSA: National Standardization Agency
$Pb(NO_3)_2$: lead(II) nitrate
pBA: polybutyl acrylate
pBA-HEMA: butyl acrylate-hydroxy ethyl methacrylate
PHXA: poly(hydroxamic acid)
pIDA: poly isododecyl acrylate
PP: photo-polymer/photo-polymerization
PVC: polyvinyl chloride
R^2: correlation coefficient
RE: reference electrode
SC: saturated calomel
SNI: Indonesian National Standard
SPE: screen-printed electrode
SSM: separated solution method
T: temperature
T_g: glass transition temperature
TGA: thermal gravimetric analysis
THFA: tetrahydrofurfuryl acrylate
THFA-co-HEMA: tetrahydro furfuryl acrylate-hydroxyl ethyl methacrylate
TP: thermo-polymerization
V: potential difference
WE: working electrode
WFD: Water Framework Directive

References

1. Ochoa GC, Cordero JCA. Effect of membrane composition and thickness on the behavior of solid contact ion selective electrodes for Pb^{2+} using a diazadibenzo-18-crown-6 ether as ionophore. ECS Trans. 2010;(1)29:361-368. https://doi.org/10.1149/1.3532332
2. Alva S, Widinugroho A, Adrian M et al. The new lead (II) ion selective electrode based on free plasticizer film of pTHFA photopolymer. J Electrochem Soc. (2019);(15)166:B1513-B1519. https://doi.org/ 10.1149/2.0601915jes

3. Ying KS, Heng LY. A screen-printed copper ion sensor with photocurable poly(n-butyl acrylate) membrane based on ionophore o-xylylene bis(N,N diisobutyldthiocarbamate), Malays J Analyt Sci. 2017;(1)21:1-12. http://dx.doi.org/10.17576/mjas-2017-2101-01
4. Wang J, Liang R, Qin W. Thin polymeric membrane ion-selective electrodes for trace-level potentiometric detection. Analyt Chim Acta.2020;1139:1-7. https://doi.org/10.1016/j.aca.2020.09.024
5. Ying KS, Heng LY et al. A new copper ionophore N1,N3-bis [[3,5-bis(trifluoromethyl)phenyl] carbamothioyl] isophtalamide for potentiometric sensor. Sains Malays. 2018;(11):2657-2666. http://dx.doi.org/10.17576/jsm-2018-4711-08
6. Bieg C, Fuchsberger K, Stelzle M. Introduction to polymer-based solid-contact ion-selective electrodes—basic concepts, practical considerations, and current research topics. Analyt Bioanalyt Chem. 2017;(1)409:45-61. https://doi.org/10.1007/s00216-016-9945-6.
7. Jackson DT, Nelson PN. Preparation and properties of some ion selective membranes: A review. J Mol Struct. 2019;1182:241-259. https://doi.org/10.1016/j.molstruc.2019.01.050
8. Heng LY, Hall EAH. Assessing a photocured self-plasticised acrylic membrane recipe for Na^+ and K^+ ion selective electrodes. Analyt Chim Acta. 2001;(1)443(1):25-40. https://doi.org/10.1016/S0003-2670(01)01195-3
9. Boruah BS, Gogoi DJ, Biswas R. Bio-inspired finger like Cu-electrodes as an effective sensing tool for heavy metal ion in aqueous solution. J Electrochem Soc. 2020;(2)167:027526. https://doi.org/10.1149/1945-7111/ab6a86
10. Shah A, Zahid A, Khan A et al. Development of a highly sensitive electrochemical sensing platform for the trace level detection of lead ions. J Electrochem Soc. 2019;(9)166:B3136-B3142. https://doi.org/10.1149/2.0271909jes
11. Sharma V, Mehata MS. Synthesis of photoactivated highly fluorescent Mn^{2+}-doped ZnSe quantum dots as effective lead sensor in drinking water. Mater Res Bull. 2021;134:111121. https://doi.org/10.1016/j.materresbull.2020.111121
12. Hao HQ, Xie L, Jin JC et al. Anionic surfactant templated hollow silica microspheres containing amino groups for the electrochemical determination of trace lead(II). J Electrochem Soc. 2016;(13)163:H1081-H1086. https://doi.org/10.1149/2.1141613jes
13. Xu R, Xiao L, Luo L et al. High electrochemical performance for Pb(II) detection based on N,S Co-doped porous honeycomb carbon modified electrodes. J Electrochem Soc. 2017;(7)164(7):B382-B389. https://doi.org/10.1149/2.0111709jes
14. Ghaedi M, Montazerozohori M, Andikaey Z et al. Fabrication of Pb^{2+} ion selective electrode based on 1-((3-((2-hydroxynaphthalen-1-yl)methyleneamino)-2,2- dimethylpropylimino) methyl) naphthalen-2-ol as new neutral ionophore. Int J Electrochem Sci. 2011;6:4127-4140.
15. Homafar A, Maleki F, Abbasi Z. Lead (II)-selective polymeric electrode using PVC membrane based on a schiff base complex of 1,2-bis(salicylidin aminooxy) ethane as an ionophore. Ener Environm Eng. 2013;(3)1:99-104. https://doi.org/10.13189/eee.2013.010301

16. Liu Y, Gao Y, Wang P. A general approach to one-step fabrication of single-piece nanocomposite membrane based Pb^{2+}-selective electrodes. Sens Actuat B Chem. 2019;281:705-712. https://doi.org/10.1016/j.snb.2018.09.113
17. Rangreez TA, Inamuddin. Synthesis and characterization of graphene Th(IV) phosphate composite cation exchanger: analytical application as lead ion-selective membrane electrode. Desalination Water Treat. 2016;57:23893-23902. https://doi.org/10.1080/19443994.2016.1138327
18. Joon NK, He N, Wagner M et al. Influence of phosphate buffer and proteins on the potentiometric response of a polymeric membrane-based solid-contact Pb(II) ion-selective electrode. Electrochim Acta. 2017;252:490-497. http://dx.doi.org/10.1016/j.electacta.2017.08.126
19. Rowdhwal SSS, Chen J. Toxic effects of di-2-ethylhexyl phthalate: an overview. Biomed Res Int. 2018. Article ID 1750368. https://doi.org/10.1155/2018/1750368
20. Anuar K, Hamdan S. A lead (II) ion selective electrode via a metal complex of poly(hydroxamic acid). Talanta.1992;(12)39:1653-1656. https://doi.org/10.1016/0039-9140(92)80199-N
21. Ulianas A, Yulkifli N, Heng LY et al. Synthesis and optimization of acrylic-N-acryloxysuccinimide copolymer microspheres. Int J Adv Sci Eng Inf Technol. 2018;(3)8:780-784. http://dx.doi.org/10.18517/ijaseit.8.3.3336
22. Lisak G, Pawlak EG, Mazurkiewicz M et al**.** New polyacrylate-based lead(II) ion-elective electrodes. Microchim Acta.2009;164:293-297. https://doi.org/10.1007/s00604-008-0089-z
23. Liu Y, Gao Y, Yan R et al. Disposable multi-walled carbon nanotubes-based plasticizer-free solid-contact Pb^{2+}-selective electrodes with a sub-ppb detection limit. Sensors. 2019;19:2550-2563. https://doi.org/10.3390/s19112550
24. Abramova N, Bratov A. Application of photocured polymer ion selective membranes for solid-state chemical sensors. Chemosensors. 2015;(2)3:190-199. https://doi.org/10.3390/chemosensors3020190
25. Michalska A, Wojciechowski M, Bulska E et al. Poly(n-butyl acrylate) based lead(II) selective electrodes. Talanta. 2009;79:1247-1251. https://doi.org/10.1016/j.talanta.2009.05.028
26. Alva S, Heng LY, Ahmad M et al. Formaldehyde biosensors in foodstuffs applying nano gold entrapped in p-HEMA deposited on screen-printed carbon electrodes: A short review. In book by Gopinath SCB, Lakshmipriya T. Nanobiosensors for biomolecular targeting. Elsevier. 2019:301-322. https://doi.org/10.1016/B978-0-12-813900-4.00013-0
27. Witjaksono G, Alva S. Applications of mass spectrometry to the analysis of adulterated food. Mass spectrometry - future perceptions and applications, Kamble GS Intech Open. 2019. http://dx.doi.org/10.5772/intechopen.84395
28. Duan G, Zhang C, Li A et al. Preparation and characterization of mesoporous zirconia made by using a poly(methyl methacrylate) template. Nanoscale Res Lett. 2008;3:118-122. https://doi.org/10.1007/s11671-008-9123-7
29. Azzahari AD, Yahya R, Hassan A et al. Synthesis and characterization of new copolymers from glycidyl methacrylate and tetrahydrofurfuryl acrylate: determination of reactivity ratios. Fibers Polym. 2012;(5)13:555-563. https://doi.org/10.1007/s12221-012-0555-4

30. Morita S. Hydrogen-bonds structure in poly(2-hydroxyethyl methacrylate) studied by T-dependent infrared spectroscopy. Front Chem. 2014;(10)2:1-5. https://doi.org/10.3389/fchem.2014.00010
31. Wan W, Jenness GR, Xiong K et al. Ring-opening reaction of furfural and tetrahydrofurfuryl alcohol on hydrogen-predosed iridium(111) and cobalt/ iridium(111) surfaces. Chem Cat Chem. 2017;9:1701-1707. http://dx.doi.org/10.1002/cctc.201601646
32. Bonilla AM, Lopez D, Garcia MF. Providing antibacterial activity to poly(2-hydroxy ethyl methacrylate) by copolymerization with a methacrylic thiazolium derivative. Int J Mol Sci. 2018;19:4120-4133. https://doi.org/10.3390/ijms19124120
33. Aouak T, Saeed WS, Al-Hafifi NM et al. Poly (2-hydroxyethylmethacrylate – co–methylmethacrylate)/lignocaine contact lens preparation, characterization, and in vitro release dynamic. Polymers. 2019;11:917-939. https://doi.org/10.3390/polym11050917
34. Lu W, Wang Y, Wang W et al. All acrylic-based thermoplastic elastomers with high upper service T and superior mechanical properties. Polym Chem. 2017;8:5741-5748. https://doi.org/10.1039/C7PY01225J
35. Vargun E, Usanmaz A. Degradation of poly(2-hydroxyethyl methacrylate) obtained by radiation in aqueous solution. J Macromol Sci. A. 2010;47:882-891. http://dx.doi.org/10.1080/10601325.2010.501304
36. Gruendken M, Velencoso MM, Hirata K et al. Structure-property relationship of low molecular weight 'liquid' polymers in blends of sulfur cured SSBR-rich compounds. Polym Test. 2020;87:106558. https://doi.org/10.1016/j.polymertesting.2020.106558
37. Ariri A, Alva S, Khaerudini DS et al. Fabrication of lead ion selective electrodes (Pb-ISE) based on poly methyl-methacrylate-co-butyl acrylate (MB28) thin film photo-polymers and pencil graphite electrodes (PGEs). Port Electrochim Acta. 2022;40:305-323. https://doi.org/10.4152/pea.2022400405
38. Chen G, Xiao S, Lorke A et al. Assessment of a solid-state phosphate selective electrode based on tungsten. J Electrochem Soc. 2018;(16)165:B787-B794. https://doi.org/10.1149/2.0101816jes
39. Panggabean AS, Preparation and characterization ion selective electrode Cd(II) based on chitosan in PVC membrane. Indones J Chem. 2011;(3)11:285-289. https://doi.org/10.22146/ijc.21394
40. Rezk MR, Fayed AS, Marzouk HM et al. Green ion selective electrode potentiometric application for the determination of cinchocaine hydrochloride in presence of its degradation products and betamethasone valerate: A comparative study of liquid and solid inner contact ion-selective electrode membranes. J Electrochem Soc. 2017;(9)164:H628-H634. https://doi.org/10.1149/2.0921709jes
41. Kozma J, Papp S, Gyurcsanyi RE. Solid-contact ion-selective electrodes based on ferrocene-functionalized multi-walled carbon nanotubes. Electrochem Commun. 2021;123:106903-106907. https://doi.org/10.1016/j.elecom.2020.106903
42. Kondratyeva YO, Solovyeva EV, Khripoun GA et al. Non-constancy of the bulk resistance of ionophore-based ion-selective electrode: A result of electrolyte co-extraction or of something else? Electrochim Acta. 2018; 259:458-465. https://doi.org/10.1016/j.electacta.2017.10.176

43. Gomez JJ, Silva MTR, Romo MR et al. Ion-selective electrodes for mercury determination at low concentrations: Construction, optimization and application. J Electrochem. Soc.2016;(3)163:B90-B96. https://doi.org/10.1149/2.0621603jes
44. Hussien EM, Derar AR. Selective determination of diclofenac and clomiphene with a single planar solid-state potentiometric ion selective electrode. J Electrochem Soc. 2019;(10)166:B780-B786. https://doi.org/10.1149/2.0701910jes
45. IUPAC. Potentiometric selectivity coefficients of ion-selective electrodes: Part 1. Inorganic cations. Pure Appl Chem. 2000;(10) 72:1851-2082. http://dx.doi.org/10.1351/pac200072101851
46. Perez MDLAA, Pedram MY. Behavior of a polymeric liquid membrane ion-selective electrode for chloride ion. J Chil Chem Soc. 2013;(4)58:1957-1958. http://dx.doi.org/10.4067/S0717-97072013000400009
47. E. Zdrachek E, Bakker E Time-dependent determination of unbiased selectivity coefficients of ion-selective electrodes for multivalent ions. Analyt Chem. 2017; 89:13441-13448. https://doi.org/10.1021/acs.analchem.7b03726
48. El-Rahman MKA, Sayed RA, El-Masry MS et al. Development of potentiometric method for *in sit*u testing of terbinafifine HCl dissolution behavior using liquid inner contact ion-selective electrode membrane. J Electrochem Soc. 2018;(3)165:B143-149. https://doi.org/10.1149/2.0091805jes
49. Ceresa A, Bakker E, Hattendorf B et al. Potentiometric polymeric membrane electrodes for measurement of environmental samples at trace levels: New requirements for selectivities and measuring protocols, and comparison with ICPMS. Analyt Chem. 2001;73:343-351. https://doi.org/10.1021/ac001034s
50. Arida, HA, Al-haddad AS, Schoning MJ. New solid-state organic membrane based lead-selective micro-electrode. Int J Electrochem Sci. 2011;6:3858 - 3867.
51. Yu S, Li F, Yin T et al. A solid-contact Pb^{2+}-selective electrode using poly(2-methoxy-5-(2-ethylhexyloxy)-p-phenylene vinylene) as ion to-electron transducer. Analyt Chim Acta. 2011;702:195-198. https://doi.org/10.1016/j.aca.2011.06.049
52. Macca C. Response time of ion-selective electrodes Current usage versus IUPAC recommendations. Analyt Chim Acta. 2004;512:183-190. https://doi.org/10.1016/j.aca.2004.03.010
53. Khan A, Baig U. Electrically conductive membrane of polyaniline–titanium(IV)phosphate cation exchange nanocomposite: Applicable for detection of Pb(II) using its ion-selective electrode. J Ind Eng Chem. 2012;18:1937-1944. http://dx.doi.org/10.1016/j.jiec.2012.05.008
54. Mashhadizadeh MH, Khani H, Shockravi A et al. Determination of ultra-trace levels of lead (II) in water samples using a modifified carbon paste electrode based on a new podand. Mater Sci Eng C. 2011;31:1674-1680. https://doi.org/10.1016/j.msec.2011.07.021
55. Sadeghi S, Dashti GR, Shamsipur M. Lead-selective poly(vinyl cholride) membrane electrod based on piroxicam as a neutral carrier. Sens Actuat B Chem. 2002;81:223-228. https://doi.org/10.1016/S0925-4005(01)00956-X

56. Wardak C. A highly selective lead-sensitive electrode with solid contact based on ionic liquid. J. Hazard. Mater. 2011;186:1131-1135. https://doi.org/10.1016/j.jhazmat.2010.11.103
57. Zeng X, Jiang W, Waterhouse GIN et al. Stable Pb(II) ion-selective electrodes with a low detection limit using silver nanoparticles/polyaniline as the solid contact. Microchim Acta. 2021;188:393. https://doi.org/10.1007/s00604-021-05046-y
58. Wardak C, Morawska K, Bator BP et al. Improved lead sensing using a solid-contact ion-selective electrode with polymeric membrane modified with carbon nanofibers and ionic liquid nanocomposite. Materials. 2023;16:1003. https://doi.org/10.3390/ma16031003
59. Nisah K, Rahmi R, Ramli M et al. Optimization of castor oil-based ion selective electrode (ISE) with active agent 1,10–phenanthroline for aqueous Pb^{2+} analysis. Membranes. 2022;12:987. https://doi.org/10.3390/membranes12100987
60. Rumanta M. Analysis of lead (Pb) pollution in the river estuaries of Jakarta Bay. The sustainable city IX: Urban regeneration and sustainability, edited by Marchettini N, Brebbia CA, Pulselli R et al. WIT Transactions on Ecology and The Environment. 2014;(2)191:1555-1564. https://doi.org/10.2495/SC141322
61. Dsikowitzky L,Wulp SAVD, Dwiyitno, et al. Transport of pollution from the megacity Jakarta into the ocean: Insights from organic pollutant mass fluxes along the Ciliwung River Estuary Coast. Shelf Sci. 2018;215:219-228, https://doi.org/10.1016/j.ecss.2018.10.017
62. Cordova MR, Riani E, Shiomoto A. Microplastics ingestion by blue panchax fish (*Aplocheilus sp*.) from Ciliwung Estuary, Jakarta, Indonesia. Mar Pollut Bull. 2020; 161:111763. https://doi.org/10.1016/j.marpolbul.2020.111763